

LONG-TERM WASTE PACKAGE DEGRADATION STUDIES AT THE YUCCA MOUNTAIN POTENTIAL HIGH-LEVEL NUCLEAR WASTE REPOSITORY

K.G. Mon, B.E. Bullard, D.E. Longsine, S. Mehta
Duke Engineering & Services
1180 Town Center Drive, Las Vegas, Nevada 89144

J. H. Lee
Sandia National Laboratories
1180 Town Center Drive, Las Vegas, Nevada 89144

A. M. Monib
Bechtel SAIC Company, LLC
1180 Town Center Drive, Las Vegas, Nevada 89144

ABSTRACT

The Site Recommendation (SR) process for the potential repository for spent nuclear fuel (SNF) and high-level nuclear waste (HLW) at Yucca Mountain, Nevada is underway. Fulfillment of the requirements for substantially complete containment of the radioactive waste emplaced in the potential repository and subsequent slow release of radionuclides from the Engineered Barrier System (EBS) into the geosphere will rely on a robust waste container design, among other EBS components. Part of the SR process involves sensitivity studies aimed at elucidating which model parameters contribute most to the drip shield and waste package degradation characteristics. The model parameters identified included (a) general corrosion rate model parameters (temperature-dependence and uncertainty treatment), and (b) stress corrosion cracking (SCC) model parameters (uncertainty treatment of stress and stress intensity factor profiles in the Alloy 22 waste package outer barrier closure weld regions, the SCC initiation stress threshold, and the fraction of manufacturing flaws oriented favorably for through-wall penetration by SCC). These model parameters were reevaluated and new distributions were generated. Also, early waste package failures due to improper heat treatment were added to the waste package degradation model. The results of these investigations indicate that the waste package failure profiles are governed by the manufacturing flaw orientation model parameters and models used.

INTRODUCTION

The SR process for the potential repository for SNF and HLW at Yucca Mountain, Nevada is underway (1). Fulfillment of the requirements for substantially complete containment of the radioactive waste emplaced in the potential repository and subsequent slow release of radionuclides from the Engineered Barrier System (EBS) into the geosphere will rely on a robust waste container design, among other EBS components. The SR waste package design (Figure 1) consists of two layers: a 20-mm-thick Alloy 22 outer barrier and a 50-mm-thick 316NG stainless steel inner shell. A Titanium Grade 7 drip shield is placed over the waste package at the time of repository closure. No backfill material is used. Although the stainless steel inner shell provides structural stability to the Alloy 22 outer barrier, no other performance credit is taken for the inner shell. The waste package outer barrier has two Alloy 22 closure lids: one 25-mm-thick outer lid

and one 10-mm-thick middle lid. The lids are welded to the outer barrier after the waste form is loaded.

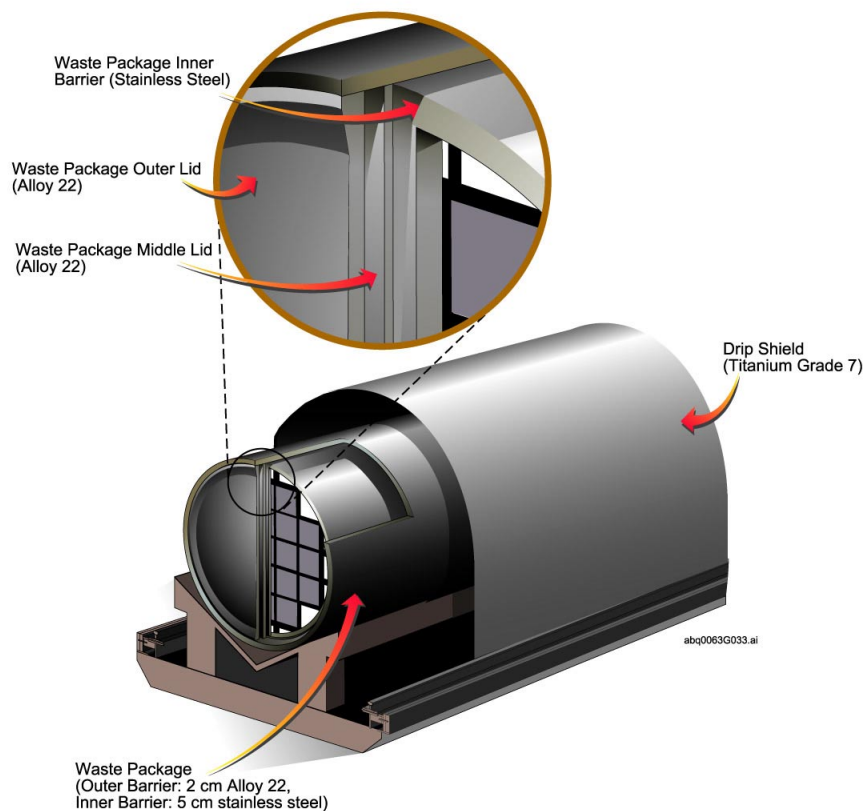


Fig. 1. Schematic Diagram of the Site Recommendation Drip Shield and Waste Package Design.

The Integrated Waste Package DEgradation (WAPDEG) stochastic simulation model (2) was used in this study to analyze long-term degradation of materials. The WAPDEG model simulates several material degradation modes, including general corrosion, localized corrosion, and SCC. The current model also includes effects of microbiologically influenced corrosion, aging and phase stability, and manufacturing flaws. The WAPDEG degradation models use the temperature and relative humidity at the drip shield and waste package surfaces as a function of time and bounding estimates of the chemistry of aqueous solutions that could form in the potential repository. WAPDEG simulation results are obtained using multiple realizations of uncertain parameters. Time histories of the type of penetrations (i.e., SCC cracks, pits, and larger general corrosion openings) and number of penetrations in the drip shields and waste packages are outputs generated by the model. These data are used to calculate both the seepage flux that can eventually contact the waste form and the amount of waste form available for release.

Part of the SR process involves sensitivity studies aimed at elucidating which model parameters contribute most to the drip shield and waste package degradation characteristics. The model parameters identified included (a) general corrosion rate model parameters (temperature-

dependence and uncertainty treatment), and (b) SCC model parameters (uncertainty treatment of stress and stress intensity factor profiles in the Alloy 22 waste package outer barrier closure weld regions, the SCC initiation stress threshold, and the fraction of manufacturing flaws oriented favorably for through-wall penetration by SCC). These model parameters were reevaluated and new distributions were generated through consideration of the results of supplemental scientific analyses. Also, early waste package failures resulting from potential improper heat treatment were added to the waste package degradation model. The results of these investigations are presented in this study. More detailed descriptions of the WAPDEG model can be found elsewhere (2).

GENERAL CORROSION

General corrosion is the relatively uniform thinning of materials without significant localized corrosion. Three types of general corrosion processes are considered: (1) dry oxidation, (2) humid-air corrosion, and (3) aqueous-phase corrosion. Dry oxidation (dry-air corrosion) occurs at a relative humidity (RH) below the threshold RH for initiation of humid-air corrosion. Dry-air corrosion is expected to have no significant impact on waste package and drip shield performance and is therefore not modeled. Humid-air corrosion occurs when the RH is high enough for the formation of a stable water film thick enough to support corrosion processes. Aqueous-phase corrosion requires the presence of bulk water resulting from dripping water percolation into the emplacement drifts. In the SR analyses, a carbonate-base water was considered the most likely to contact the drip shield and waste package surfaces.

The distributions of general corrosion rates for Alloy 22 and Titanium Grade 7 used in the WAPDEG model are based on weight-loss data from Lawrence Livermore National Laboratory's (LLNL's) Long-Term Corrosion Test Facility (LTCTF) collected after a two-year exposure period (3). The LTCTF uses three types of general corrosion samples: fully submerged, water-line (or half submerged), and samples in the vapor-phase above the solutions. The four solutions used have chemical compositions based on concentrated J-13 well water (3). J-13 well water is obtained from a well located near the potential repository and is representative of seepage water composition contacting the drip shield and waste package surfaces. The solutions vary in pH between 2.7 and 8.1 and have chloride-ion concentrations in the range of 67 to 1.284×10^5 mg/L. Specimens were tested at two temperatures (60 and 90°C) in each solution.

The corrosion data for Alloy 22 and Titanium Grade 7 indicate that the general corrosion rates for humid-air and aqueous-phase corrosion are about the same. For this reason, only one threshold RH for initiation of general corrosion is used. The threshold RH is based on the deliquescence point of sodium nitrate salt. The LTCTF data also show little sensitivity to water chemistry or exposure temperature for the water chemistry and temperature ranges considered in the test program (3). The general corrosion rates were corrected for the effects of silica scale deposition, which was estimated to increase the general corrosion rate by as much as $0.063 \mu\text{m}/\text{yr}$. The cumulative distribution function for the general corrosion rate of Alloy 22 is shown in Figure 2, which was developed for the supplemental scientific analyses discussed below, at the 60°C temperature.

Site Recommendation Treatment of General Corrosion

In the SR simulations, general corrosion is modeled with a simple linear model, (i.e., $\text{Depth} = \text{Rate} \times \text{Time}$) with no rate dependence on exposure temperature or chemical environment. Uncertainty in the general corrosion rate was treated using the Gaussian Variance Partitioning (GVP) sampling scheme (3). GVP starts with a distribution that involves both uncertainty and variability (e.g., a general corrosion distribution) and then works backward to obtain two separate distributions, one that characterizes variability and another that characterizes uncertainty. Each distribution has only a fraction of the starting distribution's total variance (i.e., if the fraction of variance due to uncertainty is U , then the fraction due to variability is $1-U$). The median value of the variability distribution is sampled from the uncertainty distribution.

In the SR simulations, the fraction of the starting distribution's total variance due to uncertainty (U) was considered to be uncertain and sampled from a uniform distribution between 0 and 1. The cumulative probability at which to sample the uncertainty distribution to obtain the median value of the variability distribution (m) was also considered uncertain and sampled from a uniform distribution between 0 and 1. Details of the GVP technique are described in more detail elsewhere (3).

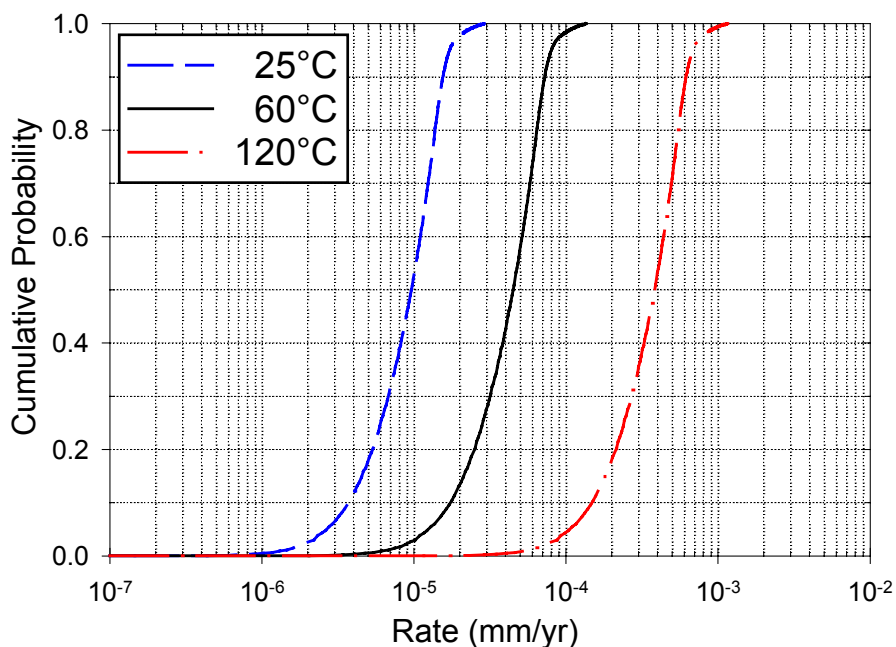


Fig. 2. Alloy 22 General Corrosion Rate Distributions at 25, 60, and 125°C.

Supplemental Science and Performance Assessment Treatment of General Corrosion

In the supplemental scientific analyses, general corrosion of the Alloy 22 waste package outer barrier was modeled assuming an Arrhenius temperature dependence (4). It was assumed that the general corrosion rate distribution used in the SR analyses (3) was representative for an exposure temperature of 60°C. The rate at any other temperature is determined by the Arrhenius equation,

given a slope term (or activation energy). The Arrhenius equation for the general-corrosion rate is:

$$R = \exp\left[c_0 - \frac{c_1}{T}\right] \quad (\text{Eq. 1})$$

where R is the general-corrosion rate, T is the temperature (Kelvin), c_0 is the intercept term, and c_1 is the slope term. Assuming the slope term is known, the intercept term is determined from the rate sampled from the LTCTF general corrosion rate distribution (R_o) by the equation:

$$c_0 = \ln(R_o) + \frac{c_1}{T_o} \quad (\text{Eq. 2})$$

where T_o is 333.15 K (60°C).

The slope term was determined by analysis of passive current density data from potentiodynamic polarization experiments for Alloy 22 (4). The tests were performed on air-aged Alloy 22 crevice specimens at pH levels of 2.75 and 7.75 and temperatures of 80, 85 and 95°C. All specimens were exposed to a undeaerated (without air or nitrogen purging) aqueous environment containing LiCl, Na₂SO₄, and NaNO₃, with Cl⁻ / (SO₄²⁻ + NO₃⁻) ratios of 10 to 1 and 100 to 1. The passive dissolution rates (i.e., general corrosion rates) were calculated from the measured passive current density using Faraday's law. The slope term was evaluated by linear regression (5). A value of 4372.96 K for the slope term was determined. Dividing the slope term by the universal gas constant results in the more familiar activation energy slope measure of about 36 kJ/mole. Plots of the Alloy 22 general corrosion rate CDFs at various temperatures are shown in Figure 2. No temperature dependence was applied to the Titanium Grade 7 general corrosion rates used.

For supplemental scientific analyses, the variances of the Alloy 22 and Titanium Grade 7 general corrosion rate distributions were considered to be solely due to uncertainty (5). The GVP sampling scheme was not used. Instead, a single general corrosion rate for each alloy exposure condition (humid-air, aqueous-phase, in-package) was sampled for use in a given realization.

STRESS CORROSION CRACKING

SCC of materials may occur when an appropriate combination of material susceptibility, tensile stress, and environment is present. SCC is assumed to occur only in the regions around the closure welds of the Alloy 22 waste package outer barrier because the residual stress in these welds cannot be relieved by processes such as bulk annealing which could damage the waste form. All residual stresses in the drip shield and waste package outer barrier, with the exception of the closure-lid weld region, can be fully stress relieved. SCC of the drip shield is possible under the applied stresses resulting from rockfall; however, SCC of the drip shield is of low consequence to drip shield (and waste package) performance, so it is not modeled. The effect of rockfall on the waste package is excluded from consideration because of the protection provided by the drip shield.

The SCC model used is based on the slip-dissolution mechanism at the crack tip for crack initiation and propagation. Although the slip dissolution model assumes that crack growth can initiate at any surface defect (e.g., a grain boundary junction, scratch, etc.) that can generate a positive stress intensity factor, a review of the relevant SCC literature (6, 7) indicates that there is a threshold stress below which SCC will not initiate on a “smooth” surface. On this basis, a threshold stress for crack initiation was used. SCC is initiated only if the threshold stress is exceeded and the stress intensity factor is greater than zero.

It has been shown that an effective approach to eliminate or delay the onset of SCC is to implement a post-welding stress mitigation process to either remove residual tensile stresses in the weld region or reduce them below threshold values for SCC initiation and growth. The closure of the waste package outer barrier is designed to include two lids (outer and middle), both Alloy 22, with two separate post-welding stress mitigation processes: local induction annealing stress relief of the outer closure-lid weld region and laser peening of the middle lid closure-weld region. The mitigation processes result in the formation of compressive surface layers and thus delay the onset of SCC until these compressive layers are removed by general corrosion processes. The post-mitigation stress and stress intensity profiles are shown as the medians in Figure 3. As discussed in the *Waste Package Degradation Process Model Report* (3), the hoop stress is the dominant stress driving crack growth through the thickness of the closure weld region. Figure 3 also shows curves related to the uncertainty treatment of the stress and stress intensity profile which are discussed below.

The slip dissolution model for stress corrosion cracking calculates the crack propagation rate, V , as a function of the local exposure environment (represented by parameter n for the repassivation rate [or repassivation slope] at the crack tip) and the stress intensity factor, K_I (3):

$$V = \bar{A}(K_I)^{\bar{n}} \quad (\text{Eq. 3})$$

where V is the crack growth rate in mm/s and K_I is the stress intensity factor in MPa (m)^{1/2}. Parameters \bar{A} and \bar{n} in the above equation are expressed in terms of the repassivation rate, n , as follows:

$$\bar{A} = 7.8 \times 10^{-2} n^{3.6} (4.1 \times 10^{-14})^n \quad (\text{Eq. 4})$$

$$\bar{n} = 4n \quad (\text{Eq. 5})$$

The slip dissolution model has been used successfully in the boiling water reactor industry as a crack propagation prediction tool (8). The residual stress and corresponding stress intensity factor are important parameters in the stress corrosion cracking analysis for the slip dissolution model (3).

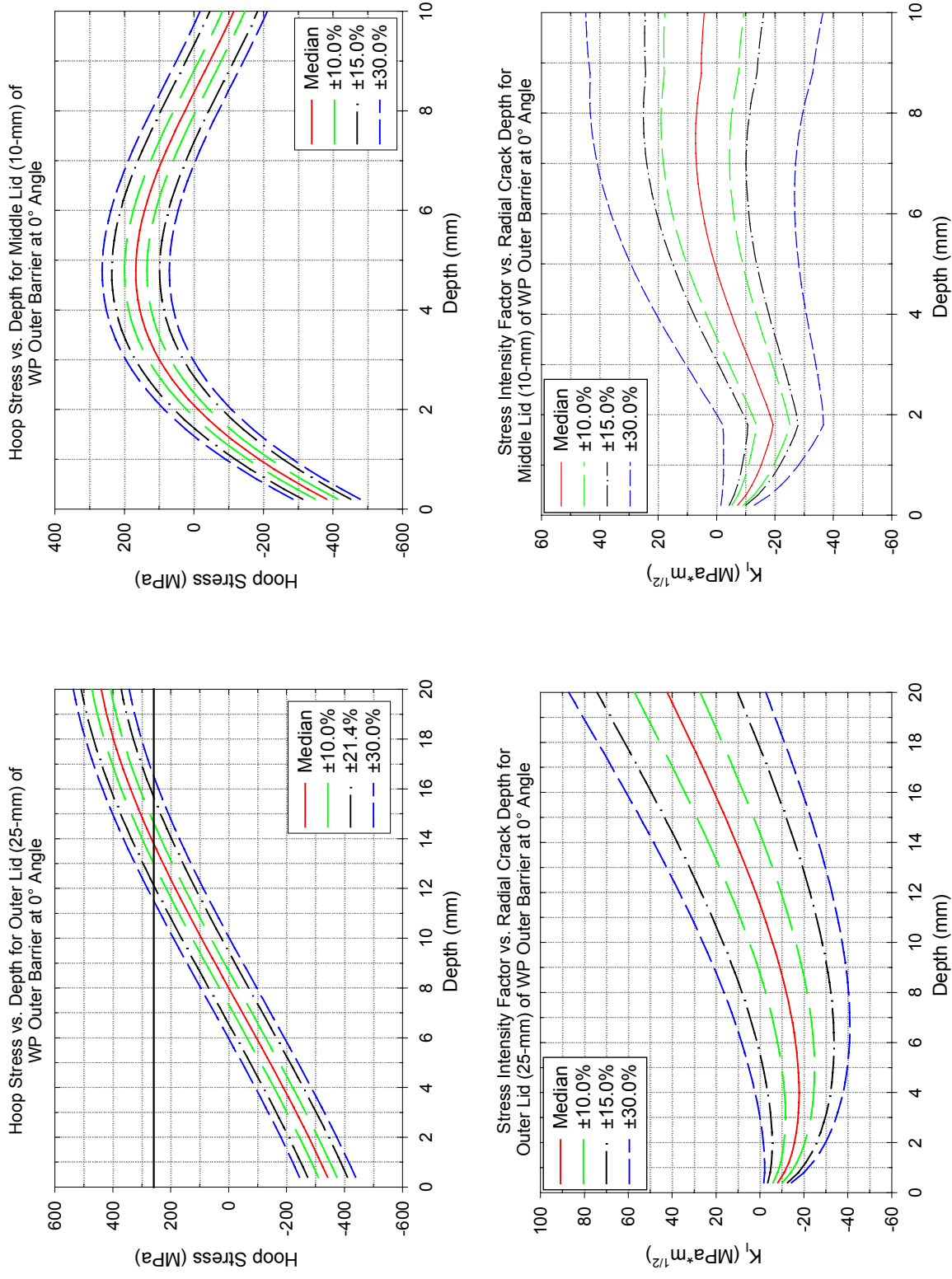


Fig. 3. Post-Mitigation Stress and Stress Intensity Profiles for the Waste Package (WP) Outer and Middle Closure Lid Weld Regions. The Horizontal Line on the Stress Profile Plots Represents 80 Percent of Yield Strength.

Site Recommendation Treatment of Repassivation Rate

In the slip-dissolution model, the rate of repassivation at the crack tip is represented by the parameter n , also referred to as the repassivation slope. A characteristic of the slip dissolution (or film rupture model) is that SCC crack growth rate decreases with increasing values of n (3). In the SR analyses, limited data were available under repository conditions and the value of n was evaluated based on data for stainless steel in boiling water reactors (3). Because stainless steels are more prone to stress corrosion cracking than Alloy 22, the parameter estimates are considered conservative. In the SR analyses (2), n is represented by a uniform distribution with an upper bound of 0.84 and a lower bound of 0.75, and the variation of the parameter value is assumed to be entirely due to uncertainty.

Supplemental Science and Performance Assessment Treatment of Repassivation Rate

From recently obtained longer-term data for Alloy 22 under repository-relevant conditions, the model parameter n and its uncertainty have been reevaluated. The parameter is now represented by a uniform distribution with an upper bound of 0.920 and a lower bound of 0.843 (5). As in the SR analyses, variation in the parameter value is assumed to be entirely due to uncertainty. With the updated uncertainty distribution for n , the through-wall penetration time of a 20-mm-thick Alloy 22 layer by SCC would increase significantly relative to the SR analyses (3).

Site Recommendation Treatment of Stress and Stress Intensity Factor Profiles

In SR analyses, the hoop stress (σ_s in MPa) as a function of depth (x in mm) is given by a third order polynomial equation of the form (2):

$$\sigma_s(x) = A_0 + A_1 \cdot x + A_2 \cdot x^2 + A_3 \cdot x^3 \quad (\text{Eq. 6})$$

The values of the coefficients (A_i 's) used in the model are given in Table I (2).

Table I. Stress Coefficients Used in the Evaluation of Stress Profiles for the Outer and Middle Closure Lids of Waste Package.

Coefficient	Outer Closure Lid	Middle Closure Lid
A_0	-356.30449	-437.720543
A_1	37.188256	176.967239
A_2	1.435966	-15.606072
A_3	-0.065277	0.367099

The hoop stress state was determined to vary with angle (θ) around the circumference of the waste package closure-lid welds ($\theta = 0$ point arbitrarily chosen) according to the following functional form (2):

$$\sigma_t(x, \theta) = \sigma_s(x) - (17.236892) \cdot (1 - \cos(\theta)) \quad (\text{Eq. 7})$$

Note that σ_s (defined in Eq. 9) uses the stress coefficients (A_i) defined in Table I. Based on the angular stress variation in Eq. 10, the stress intensity factor variation with angle is given by (2):

$$K_t(x, \theta) = K_s(x) \cdot \left(\frac{\sigma_t(\text{Thck}, \theta)}{\sigma_t(\text{Thck}, 0)} \right) \quad (\text{Eq. 8})$$

where $Thck$ is the lid thickness and $K_s(x)$ is the median stress intensity factor profile shown in Figure 3.

In SR, the uncertainty in the stress state and stress intensity factor is introduced through a scaling factor, sz , which was sampled from a triangular distribution with a mode of zero, and symmetric upper and lower bounds of ± 0.30 for both waste package closure lids (2). Thus, for a given realization, the stress profile is given by:

$$\sigma(x, \theta) = \sigma_i(x, \theta) + sz \cdot YS \quad (\text{Eq.9})$$

where YS is the yield strength. The stress intensity factor relation is given by:

$$K(x, \theta) = K_i(x, \theta) + 0.058534 \cdot sz \cdot YS \cdot \sqrt{\pi \cdot x} \quad (\text{Eq.10})$$

In Figure 3, symmetric upper and lower bounds for sz of ± 0.10 , 0.15 (Middle Lid) or 0.214 (Outer Lid), and ± 0.30 are shown for comparison.

Supplemental Science and Performance Assessment Treatment of Stress and Stress Intensity Factor Profiles

In the supplemental scientific analyses, the same median stress and stress intensity factor profiles (Figure 3) were used, however, different upper and lower bounds for the sz distribution were used for each closure-lid weld region. For the outer closure-lid, consideration of literature data (9 - 11) resulted in a revision of the symmetric upper and lower bounds of sz from ± 0.30 to ± 0.214 .

For the inner closure-lid, consideration of literature data resulted in the development of a cumulative distribution function for the symmetric upper and lower bounds on sz . The literature data consisted of X-ray diffraction measurements of residual stresses in shot-peened Incoloy 908 samples (12). A measurement error was estimated for each measurement which was used to weight the residual stress measurements in estimating the mean and standard deviation of the residual stress state (5). These measures were then used to determine the cumulative distribution function for the symmetric upper and lower bounds on sz . The use of data obtained for shot-peened Incoloy 908 is appropriate for this application because Incoloy 908 is a nickel-based alloy similar to Alloy 22 and shot peening is an analogous process to laser peening. For each realization, the symmetric upper and lower bounds of sz for the waste package middle closure lid weld region were sampled from a distribution (5):

$$\pm \frac{0.5978}{\sqrt{\chi^2(16)}} \quad (\text{Eq. 11})$$

where $\chi^2(16)$ is the chi-square distribution with 16 degrees of freedom.

Site Recommendation Treatment of SCC Initiation Stress Threshold

For SR simulations, the SCC initiation stress threshold is conservatively estimated to be in the range of 20 to 30 percent of the yield strength based on data for stainless steels (3). For SR, all

of the parameters for the slip dissolution model are based on data for stainless steel. Because stainless steels are much more prone to SCC than Alloy 22, these parameter estimates are considered to be conservative when used to model SCC of Alloy 22.

Supplemental Science and Performance Assessment Treatment of SCC Initiation Stress Threshold

In the supplemental scientific analyses, a detailed review of literature data (6, 7) and recent Yucca Mountain Project results (5) revealed the initiation stress threshold values for high nickel-content stainless steels and nickel-base alloys may well exceed the yield strength. Alloy 22 U-bend (10 to 15 percent strain) specimen data obtained in boiling magnesium chloride solutions indicate the SCC initiation stress threshold may exceed 200 percent of the yield strength (6, 7). Yucca Mountain Project data has been obtained under a variety of metallurgical conditions, exposure environments, and loading profiles (5). Analysis of this data led to the conclusion that the SCC initiation stress threshold should be sampled from a uniform distribution between 80 and 90 percent of the yield strength. The stress profile plots for the waste package outer barrier shown in Figure 3 have a horizontal line representing the 80 percent of yield strength line (~260 MPa). For the waste package outer lid, SCC initiation will be delayed until at least 11 mm of thickness have been removed by general corrosion processes. For the waste package middle closure lid, for all but the most extreme stress profiles, SCC will not initiate.

MANUFACTURING FLAWS IN CLOSURE WELDS

Preexisting manufacturing flaws in the waste package closure-lid welds are likely sites for SCC. Manufacturing flaws are generally larger than other surface defects and are conservatively modeled as maintaining their depth relative to the advancing general corrosion front (i.e., they are not removed by general corrosion processes). Therefore, the characteristics of flaws in the waste package closure welds are important inputs to the waste package SCC analysis. As discussed earlier, residual stress analyses showed that the hoop stress is the dominant stress driving crack growth; thus, only radially-oriented flaws are potential sites for SCC.

Site Recommendation Treatment of Manufacturing Flaws in Closure Welds

In the SR analyses, the frequency and size distributions for manufacturing flaws in the closure welds were developed based on published data for stainless steel pipe welds in nuclear power plants (13). The published data used to develop the manufacturing defect model are those utilizing welding techniques and post-weld inspection methods that are relevant to waste package manufacturing (13). The SR analyses (2) conservatively assumed that all manufacturing flaws are oriented in such a way that they could grow in the radial direction under the action of residual hoop stresses (2).

Supplemental Science and Performance Assessment Treatment of Manufacturing Flaws in Closure Welds

In the supplemental scientific analyses, based on consideration of additional literature information and limited measured data from the Yucca Mountain Project waste package mock-ups, analyses were conducted to quantify the orientation of weld flaws in the waste package closure welds. Only two weld methods are being considered for the waste package fabrication process, gas metal arc and tungsten inert gas methods. These welding processes are designed to

eliminate slag inclusions, a common flaw in other welding techniques. The most common flaws for gas metal arc and tungsten inert gas are lack of fusion flaws due to missed side wall or lack of penetration in the side wall. Flaws resulting from the lack of fusion are, by definition, oriented in the direction of the weld bead (i.e., oriented circumferentially not radially) (14). Analysis of waste package mock-ups revealed no radially oriented flaws (15). Shcherbinskii and Myakishev (16) describe a statistical treatment of weld flaw orientations based on analysis of a significant data set of flaw orientation measurements and conclude that planar-type weld flaws, detected ultrasonically, tend to be predominately oriented parallel to the direction of the weld centerline. More than 98 percent of the flaws detected fall within ± 16 degrees of the weld center line in the case of steam pipe welds. A similar conclusion, drawn from the data for plate welds (16), indicates that the statistical distribution of the flaw angle with respect to the weld centerline can be approximated with a centered normal distribution with a maximum standard deviation of 5 degrees. This yields a probability of 99 percent that a flaw is oriented within about ± 13 degrees of the weld centerline. Based on these analyses it was determined (5) that the fraction of flaws capable of propagation in the radial direction could be sampled from a lognormal distribution with a mean of one percent, an upper bound of 50 percent, and lower bound of 0.02 percent.

EARLY WASTE PACKAGE FAILURE: IMPROPER HEAT TREATMENT

Site Recommendation Treatment of Early Waste Package Failure

An extensive literature review was conducted for the *Total System Performance Assessment for the Site Recommendation* (TSPA-SR) (1) to collect information to develop scenarios and conditions that could lead to early failure of waste packages. From this literature review and analysis, a number of potential mechanisms were identified that could lead to early waste package failures under repository conditions (13). Those mechanisms were further evaluated to develop the probability of their occurrence and the consequence of the mechanism to waste package failures under repository conditions (13). Of all mechanisms considered, only weld flaws in the waste package closure welds were found to have a significant probability of occurrence.

Supplemental Science and Performance Assessment Treatment of Early Waste Package Failure

In the supplemental scientific analyses, the potential early failure mechanisms in the *Analysis of Mechanisms for Early Waste Package Failure* (13) were reevaluated (5). It was concluded that improper heat treatment of waste packages needs to be included in the waste package performance analysis. The consequence of improper heat treatment could be a gross failure of affected waste packages, although the probability of this occurrence is very low. The results of the analysis were that the expected number of improperly heat-treated waste packages per realization is 0.263 (5). Using this value as the mean of a Poisson distribution, there is a 76.9 percent chance that no single waste package is improperly heat-treated in a given realization of the potential repository. The probability of having at least one waste package improperly heat-treated is 20.2 percent, and the probability of having two waste packages affected is 2.6 percent. In evaluating consequences of potential improper heat treatments, a nonmechanistic failure of the outer and inner closure lids of the waste package outer barrier was assumed (i.e., it

was conservatively assumed that a large area was failed immediately upon initiation of general corrosion) (5).

INTEGRATED WASTE PACKAGE DEGRADATION MODEL

Model Inputs and General Description

Inputs to the WAPDEG Model (2) include:

- Temperature, relative humidity, and pH environments on the drip shield and waste package surfaces as a function of time
- A RH threshold for degradation initiation which is a function of exposure temperature based on the deliquescence point of NaNO_3 salt, which is conservatively assumed to be always present on the waste package and drip shield surface at all times.
- General corrosion rates based on experimental data collected from LLNL's LTCTF.
- Stress and stress intensity factor profiles for the outer and middle closure lid regions
- SCC initiation and propagation rate parameters.
- Number, size, and orientation of manufacturing defects in waste package outer barrier closure-lid welds and their effect on SCC.

The WAPDEG Model (2) was executed for 300 realizations of the uncertain input parameters for 400 drip shield/waste package pairs per realization. The WAPDEG Model uses a stochastic approach to capture the effects of variability of exposure conditions across the potential repository and of degradation processes on a single waste package. Spatial variability is represented by dividing the waste package and drip shield surface into subareas called "patches" and distributing the corrosion rates and model parameter values stochastically over the patches. All degradation modeling occurs at the patch level. 500 patches were used to simulate the drip shields and 1,000 patches were used to simulate the waste packages (2). Variability in waste package degradation across the repository is modeled either by incorporating explicitly the spatial distribution of the exposure conditions or by stochastically varying the corrosion model parameters over the drip shields/waste packages to be simulated and the patches in each drip shield/waste package.

Three types of drip shield or waste package failure openings are possible in the WAPDEG software: patch openings (due to general corrosion processes), pit openings (due to localized corrosion), and crack openings (due to SCC). Neither the drip shield nor the waste package are subject to localized corrosion processes under the exposure conditions in the potential repository (2). The drip shield and waste package outer shell are fully stress relief annealed (with the exception of the waste package closure lid welds) and are thus not subject to SCC. Thus, the only degradation mode modeled for the drip shield is general corrosion leading to patch failures. The waste package is subject to general corrosion and SCC in the closure-lid weld regions only.

WAPDEG Model Results

The results of calculations using the WAPDEG Model consist of time histories of the type and number of drip shield and waste package penetrations. For the purposes of this study, it is sufficient to discuss only the waste package first penetration profiles as shown in Figure 4. Each of the plots in Figure 4 represent the mean waste package failure profile generated from consideration of 300 realizations of the uncertain model parameters. In Figure 4, WAPDEG mean first penetration profiles are shown for the TSPA-SR base case and several sensitivity studies using the Lower Temperature Operating Mode (LTOM) thermal hydrology. Except for general corrosion in the supplemental scientific analyses, no drip shield or waste package degradation models are thermal hydrology dependent. This is illustrated by the two leftmost waste package failure profiles which are nearly identical (differing only by the inclusion of the waste package early failure model in the LTOM case) although the TSPA-SR base case uses a higher temperature operating mode thermal hydrology model. These profiles show that only about 0.0025 percent of the waste packages fail due to the Early Waste Package Failure Model. For both cases, the mean fraction of waste packages failed starts to increase at about 10,000 years with 50 percent of the waste packages failing by about 95,000 years. The first waste package failures for these cases are primarily by propagation of SCC from manufacturing defect flaws in the waste package outer barrier closure-lid weld regions.

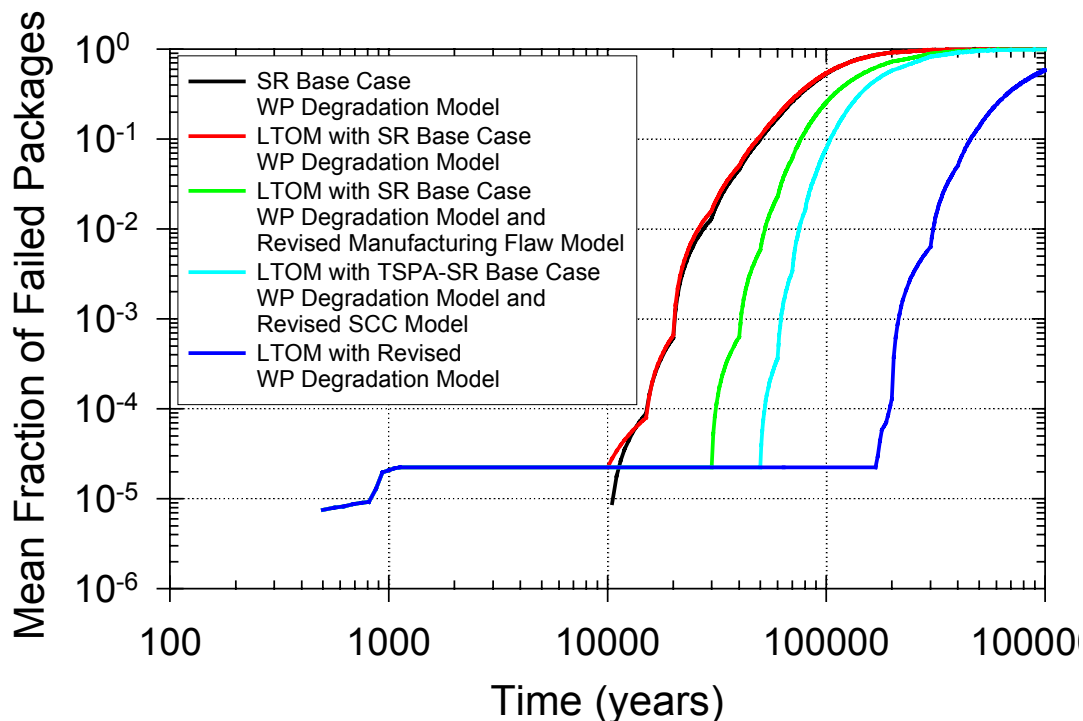


Fig. 4. Waste Package Mean Failure Fractions Using the SR Base Case Model and Sensitivities Resulting from to Supplemental Scientific Analyses.

The next earliest failing profile shows the effect of incorporating the supplemental scientific analyses of manufacturing defect orientation on waste package first penetration characteristics. For this case, the number of manufacturing flaws capable of propagating by SCC is decreased by a factor sampled from a log normal distribution with a mean of one percent, an upper bound of

50 percent, and lower bound of 0.02 percent. Waste packages that had not failed by the Early Waste Package Failure Model begin to fail at about 30,000 years with 50 percent of the waste packages failing by 140,000 years. The dominant mode of failure for these waste packages is still SCC but the failure times are significantly delayed by the decrease in the number of manufacturing flaws capable of propagation.

In the third sensitivity analysis (second curve from the right), the waste package degradation model incorporates the supplemental science analyses of manufacturing defect orientation, SCC model parameters, and the Early Waste Package Failure Model. The LTOM thermal hydrology is used. Waste packages not failed by the Early Waste Package Failure Model begin to fail at about 50,000 years with 50 percent of the waste packages failing by about 550,000 years. The failure times are significantly delayed due to the modifications to the SCC model parameters. Particularly the increase in the stress threshold for SCC initiation (see Figure 3), has eliminated any impact of SCC on waste package failure characteristics. It should be noted that manufacturing flaws penetrate before general corrosion because they are conservatively modeled to maintain their depth relative to the advancing general corrosion front (e.g., a 3 mm manufacturing flaw will penetrate the 25 mm closure-lid when the general corrosion depth reaches 22 mm), however, the number of manufacturing flaws is small. Therefore, the bulk of waste package first penetrations are by general corrosion.

The remaining analysis examines the effect of all of the supplemental scientific analyses on waste package first failure characteristics. The latest failing profile in Figure 4 includes all of the modifications discussed for the previous failure profile as well as the supplemental scientific analyses for general corrosion, i.e., temperature dependence and the assumption that all variance is due to uncertainty. Waste packages not failed by the Early Waste Package Failure Model begin to fail at about 175,000 years with 50 percent of the waste packages failing by about 880,000 years. Although some of the delay in waste package first penetration is due to the assumption that all variance in general corrosion is due to uncertainty, the bulk of the delay is due to the addition of temperature dependence. The general corrosion rates in the Arrhenius model used (Eq. 1) would be higher than those used in SR analyses when the exposure temperature is greater than 60°C, however, when the exposure temperature falls below 60°C (usually after about 10,000 years) the general corrosion rate is much lower resulting in the observed long waste package lifetimes.

CONCLUSION

In this study, results of supplemental scientific analyses of general corrosion rate model parameters and SCC model parameters were presented. Also, an Early Waste Package Failure Model was discussed. The effects of these supplemental scientific analyses on drip shield and waste package performance were assessed using the WAPDEG Model. The Early Waste Package Failure Model has little impact on waste package degradation profiles leading to the failure of only about 0.0025 percent of the waste packages in the mean case. The WAPDEG results show that incorporation of the effect of manufacturing flaw orientation has a large impact on waste package first failure profiles delaying the mean first failure time (for those waste packages not failed by the Early Waste Package Failure Model) by about 20,000 years (from 10,000 to 30,000 years). The addition of revisions to SCC model parameters (the uncertainty treatment of stress and stress intensity factor profiles in the Alloy 22 waste package outer barrier

closure weld regions, and the SCC initiation stress threshold) delayed first waste package failure (for those waste packages not failed by the Early Waste Package Failure Model) until about 50,000 years. Perhaps the strongest effect on waste package first failure profiles was exhibited by changes in the general corrosion model, particularly the addition of an Arrhenius temperature dependence. Revisions to the general corrosion model parameters delayed first waste package failure (for those waste packages not failed by the Early Waste Package Failure Model) until about 175,000 years.

REFERENCES

1. CRWMS M&O (Civilian Radioactive Waste Management System), "Total System Performance Assessment for the Site Recommendation", TDR-WIS-PA-000001 REV 00 ICN 01, Las Vegas, Nevada, CRWMS M&O (2000).
2. CRWMS M&O, "WAPDEG Analysis of Waste Package and Drip Shield Degradation", ANL-EBS-PA-000001 REV 00 ICN 01, Las Vegas, Nevada, CRWMS M&O (2000).
3. CRWMS M&O, "Waste Package Degradation Process Model Report", TDR-WIS-MD-000002 REV 00 ICN 02, Las Vegas, Nevada, CRWMS M&O (2000).
4. J. R. SCULLY, G. ILEVARE, and C. MARKS, "Passivity and Passive Corrosion of Alloys 625 and 22", SEAS Report No. UVA/527653/MSE01/103, Charlottesville, Virginia, University of Virginia, School of Engineering & Applied Science (2001).
5. BSC (Bechtel SAIC Company), "FY 01 Supplemental Science and Performance Analyses, Volume 1: Scientific Bases and Analyses", TDR-MGR-MD-000007 REV 00 ICN 01, Las Vegas, Nevada, Bechtel SAIC Company (2001).
6. M. L. ERBING FALKLAND, "Duplex Stainless Steels", Chapter 38 of Uhlig's Corrosion Handbook, Revie, R.W., ed. 2nd Edition, New York, New York, John Wiley & Sons. (2000).
7. HAYNES INTERNATIONAL, "Hastelloy C-2000 Alloy", H-2111, Kokomo, Indiana, Haynes International (1998).
8. ASM INTERNATIONAL, "Corrosion", Volume 13 of Metals Handbook, 9th Edition, Metals Park, Ohio, ASM International (1987).
9. EPRI (Electric Power Research Institute) "Induction Heating Stress Improvement", EPRI NP-3375, Palo Alto, California, Electric Power Research Institute (1983).
10. R. M. CHRENKO, "Residual Stress Measurements on Type 304 Stainless Steel Welded Pipes", Proceedings of the Seminar on Countermeasures for Pipe Cracking in BWRs, January 22-24 1980, Palo Alto, California, Paper No. 21, EPRI WS-79-174, Volume 2, Palo Alto, California, Electric Power Research Institute (1980).
11. W. J. SHACK and W. A. ELLINGSON, "Measured Residual Stresses in Type 304 Stainless Steel Piping Butt Weldments", Proceedings of the Seminar on Countermeasures for Pipe Cracking in BWRs, January 22-24 1980, Palo Alto, California, Paper No. 22, EPRI WS-79-174, Volume 2, Palo Alto, California, Electric Power Research Institute (1980).
12. V. PASUPATHI, "Documentation of Literature on Residual Stress Measurements", Interoffice Correspondence from V. Pasupathi (CRWMS M&O) to G. M. Gordon, May 19, 2000, LV.WP.VP.05/00-070, with enclosures (2000).
13. CRWMS M&O, "Analysis of Mechanisms for Early Waste Package Failure", ANL-EBS-MD-000023 REV 02, Las Vegas, Nevada, CRWMS M&O (2000).
14. CRWMS M&O, "Waste Package FY-00 Closure Methods Report", TDR-EBS-ND-000005 REV 00, Las Vegas, Nevada, CRWMS M&O (2000).

15. CRWMS M&O, "Waste Package Phase II Closure Methods Report", BBA000000-01717-5705-00016 REV 00, Las Vegas, Nevada, CRWMS M&O. (1998).
16. V. G. SHCHERBINSKII. and V. M. MYAKISHEV, "Statistical Distribution of Welding Defects with Respect to Azimuth", Translated from Defektoskopiya, No. 4, 143-144. New York, New York, Plenum Publishing (1970).

This work was performed and funded under DOE contract DE-AC08-01RW12101 for the Civilian Radioactive Waste Management System (CRWMS M&O) led by the prime contractor (Bechtel SAIC Company, LLC).